

COMPACT BLUE-GREEN LASERS

W. P. RISK
T. R. GOSNELL
A. V. NURMIKKO



CAMBRIDGE
UNIVERSITY PRESS

PUBLISHED BY THE PRESS SYNDICATE OF THE UNIVERSITY OF CAMBRIDGE
The Pitt Building, Trumpington Street, Cambridge, United Kingdom

CAMBRIDGE UNIVERSITY PRESS
The Edinburgh Building, Cambridge CB2 2RU, UK
40 West 20th Street, New York, NY 10011-4211, USA
477 Williamstown Road, Port Melbourne, VIC 3207, Australia
Ruiz de Alarcón 13, 28014 Madrid, Spain
Dock House, The Waterfront, Cape Town 8001, South Africa
<http://www.cambridge.org>

© Cambridge University Press 2003

This book is in copyright. Subject to statutory exception
and to the provisions of relevant collective licensing agreements,
no reproduction of any part may take place without
the written permission of Cambridge University Press.

First published 2003

Printed in the United Kingdom at the University Press, Cambridge

Typeface Times 11/14 pt *System* L^AT_EX 2_ε [TB]

A catalogue record for this book is available from the British Library

ISBN 0 521 62318 9 hardback
ISBN 0 521 52103 3 paperback

Contents

<i>Preface</i>	<i>page xi</i>
1 The need for compact blue-green lasers	1
1.1 A short historical overview	1
1.2 Applications for compact blue-green lasers	3
1.2.1 Optical data storage	3
1.2.2 Reprographics	5
1.2.3 Color displays	6
1.2.4 Submarine communications	8
1.2.5 Spectroscopic applications	12
1.2.6 Biotechnology	14
1.3 Blue-green and beyond	17
References	17
Part 1 Blue-green lasers based on nonlinear frequency conversion	20
2 Fundamentals of nonlinear frequency upconversion	20
2.1 Introduction	20
2.2 Basic principles of SHG and SFG	21
2.2.1 The nature of the nonlinear polarization	21
2.2.2 Frequencies of the induced polarization	23
2.2.3 The d coefficient	28
2.2.4 The generated wave	30
2.2.5 SHG with monochromatic waves	34
2.2.6 Multi-longitudinal mode sources	34
2.2.7 Pump depletion	38
2.3 Spatial confinement	43
2.3.1 Boyd–Kleinman analysis for SHG with circular gaussian beams	43
2.3.2 Guided-wave SHG	51

2.4	Phasematching	56
2.4.1	Introduction	56
2.4.2	Birefringent phasematching	57
2.4.3	Quasi-phasematching (QPM)	71
2.4.4	Waveguide phasematching	90
2.4.5	Other phasematching techniques	97
2.4.6	Summary	101
2.5	Materials for nonlinear generation of blue-green light	101
2.5.1	Introduction	101
2.5.2	Lithium niobate (LN)	101
2.5.3	Lithium tantalate (LT)	108
2.5.4	Potassium titanyl phosphate (KTP)	110
2.5.5	Rubidium titanyl arsenate (RTA)	115
2.5.6	Other KTP isomorphs	119
2.5.7	Potassium niobate (KN)	119
2.5.8	Potassium lithium niobate (KLN)	121
2.5.9	Lithium iodate	123
2.5.10	Beta barium borate (BBO) and lithium borate (LBO)	124
2.5.11	Other materials	126
2.6	Summary	130
	References	130
3	Single-pass SHG and SFG	149
3.1	Introduction	149
3.2	Direct single-pass SHG of diode lasers	151
3.2.1	Early experiments with gain-guided lasers	151
3.2.2	Early experiments with index-guided lasers	154
3.2.3	High-power index-guided narrow-stripe lasers	156
3.2.4	Multiple-stripe arrays	157
3.2.5	Broad-area lasers	160
3.2.6	Master oscillator–power amplifier (MOPA) configurations	161
3.2.7	Angled-grating distributed feedback (DFB) lasers	169
3.3	Single-pass SHG of diode-pumped solid-state lasers	170
3.3.1	Frequency-doubling of 1064-nm Nd:YAG lasers	177
3.3.2	Frequency-doubling of 946-nm Nd:YAG lasers	177
3.3.3	Sum-frequency mixing	178
3.4	Summary	178
	References	179

4	Resonator-enhanced SHG and SFG	183
4.1	Introduction	183
4.2	Theory of resonator enhancement	187
4.2.1	The impact of loss	189
4.2.2	Impedance matching	191
4.2.3	Frequency matching	193
4.2.4	Approaches to frequency locking	194
4.2.5	Mode matching	207
4.3	Other considerations	213
4.3.1	Temperature locking	213
4.3.2	Modulation	214
4.3.3	Bireflection in monolithic ring resonators	215
4.4	Summary	220
	References	220
5	Intracavity SHG and SFG	223
5.1	Introduction	223
5.2	Theory of intracavity SHG	224
5.3	The “green problem”	229
5.3.1	The problem itself	229
5.3.2	Solutions to the “green problem”	231
5.3.3	Single-mode operation	235
5.4	Blue lasers based on intracavity SHG of 946-nm Nd:YAG lasers	245
5.5	Intracavity SHG of Cr:LiSAF lasers	249
5.6	Self-frequency-doubling	250
5.6.1	Nd:LN	251
5.6.2	NYAB	252
5.6.3	Periodically-poled materials	253
5.6.4	Other materials	253
5.7	Intracavity sum-frequency mixing	253
5.8	Summary	255
	References	256
6	Guided-wave SHG	263
6.1	Introduction	263
6.2	Fabrication issues	264
6.3	Integration issues	269
6.3.1	Feedback and frequency stability	270
6.3.2	Polarization compatibility	276
6.3.3	Coupling	282
6.3.4	Control of the phasematching condition	283
6.3.5	Extrinsic efficiency enhancement	284

6.4	Summary	286
	References	287
Part 2	Upconversion lasers: Physics and devices	292
7	Essentials of upconversion laser physics	292
7.1	Introduction to upconversion lasers and rare-earth optical physics	292
7.1.1	Overview of rare-earth spectroscopy	295
7.1.2	Qualitative features of rare-earth spectroscopy	296
7.2	Elements of atomic structure	303
7.2.1	The effective central potential	303
7.2.2	Electronic structure of the free rare-earth ions	306
7.3	The Judd–Ofelt expression for optical intensities	324
7.3.1	Basic formulation	325
7.3.2	The Judd–Ofelt expression for the oscillator strength	329
7.3.3	Selection rules for electric dipole transitions	336
7.4	Nonradiative relaxation	338
7.5	Radiationless energy transfer	341
7.6	Mechanisms of upconversion	345
7.6.1	Resonant multi-photon absorption	345
7.6.2	Cooperative upconversion	348
7.6.3	Rate equation formulation of upconversion by radiationless energy transfer	357
7.6.4	The photon avalanche	360
7.7	Essentials of laser physics	363
7.7.1	Qualitative picture	364
7.7.2	Rate equations for continuous-wave amplification and laser oscillation	365
7.8	Summary	382
	References	383
8	Upconversion lasers	385
8.1	Historical introduction	385
8.2	Bulk upconversion lasers	397
8.2.1	Upconversion pumped Er^{3+} infrared lasers	398
8.2.2	Er^{3+} visible upconversion lasers	410
8.2.3	Tm^{3+} upconversion lasers	420
8.2.4	Pr^{3+} upconversion lasers	424
8.2.5	Nd^{3+} upconversion lasers	425
8.3	Upconversion fiber lasers	427
8.3.1	Er^{3+} fiber lasers; $^4S_{3/2} \rightarrow ^4I_{15/2}$ transition at 556 nm	433

8.3.2	Tm ³⁺ fiber lasers	436
8.3.3	Pt ³⁺ fiber lasers	445
8.3.4	Ho ³⁺ fiber lasers, $^5S_2 \rightarrow ^5I_8$ transition at ~ 550 nm	455
8.3.5	Nd ³⁺ fiber lasers	457
8.4	Prospects	458
	References	460
Part 3	Blue-green semiconductor lasers	468
9	Introduction to blue-green semiconductor lasers	468
9.1	Overview	468
9.2	Overview of physical properties of wide-bandgap semiconductors	470
9.2.1	Lattice matching	470
9.2.2	Epitaxial lateral overgrowth (ELOG)	472
9.2.3	Basic physical parameters	474
9.3	Doping in wide-gap semiconductors	475
9.4	Ohmic contacts for <i>p</i> -type wide-gap semiconductors	478
9.4.1	Ohmic contacts to <i>p</i> -AlGaInN	479
9.4.2	New approaches to <i>p</i> -contacts	481
9.4.3	Ohmic contacts to <i>p</i> -ZnSe: bandstructure engineering	482
9.5	Summary	484
	References	484
10	Device design, performance, and physics of optical gain of the InGaN QW violet diode lasers	487
10.1	Overview of blue and green diode laser device issues	487
10.2	The InGaN MQW violet diode laser: Design and performance	488
10.2.1	Layered design and epitaxial growth	488
10.2.2	Diode laser fabrication and performance	496
10.3	Physics of optical gain in the InGaN MQW diode laser	501
10.3.1	On the electronic microstructure of InGaN QWs	506
10.3.2	Excitonic contributions in green-blue ZnSe-based QW diode lasers	509
10.4	Summary	513
	References	513
11	Prospects and properties for vertical-cavity blue light emitters	517
11.1	Background	517
11.2	Optical resonator design and fabrication: Demonstration of optically-pumped VCSEL operation in the 380–410-nm range	518

11.2.1	All-dielectric DBR resonator	519
11.2.2	Stress engineering of AlGaIn/GaN DBRs	521
11.3	Electrical injection: Demonstration resonant-cavity LEDs	524
11.4	Summary	530
	References	530
12	Concluding remarks	533
	References	536
	<i>Index</i>	537

1

The need for compact blue-green lasers

1.1 A SHORT HISTORICAL OVERVIEW

For years after its invention in 1961, the laser was described as a remarkable tool in search of an application. However, by the late 1970s and early 1980s, a variety of applications had emerged that were limited in their implementation by lack of a suitable laser. The common thread running through these applications was the need for a powerful, compact, rugged, inexpensive source of light in the blue-green portion of the spectrum. The details varied greatly, depending on the application: some required tunability, some a fixed wavelength; some required a minuscule amount of optical power, others a great deal; some required continuous-wave (cw) oscillation, others rapid modulation.

In many of these applications, gas lasers – such as argon-ion or helium-cadmium lasers – were initially used to provide blue-green light, and in some cases were incorporated into commercial products; however, they could not satisfy the requirements of every application. The lasing wavelengths available from these lasers are fixed by the atomic transitions of the gas species, and some applications required a laser wavelength that is simply not available from an argon-ion or helium-cadmium laser. Other applications required a degree of tunability that is unavailable from a gas laser. In many of them, the limited lifetime, mechanical fragility, and relatively large size of gas lasers was a problem.

At about the same time, new options for generation of blue-green radiation began to appear, due to developments in other areas of laser science and technology. The development of highly efficient, high-power semiconductor diode lasers at wavelengths around 810 nm opened up the possibility of diode-pumping solid-state lasers, such as those based on neodymium-doped crystals and glasses. New and improved nonlinear materials made it practical to apply second-harmonic generation to the infrared outputs of these diode-pumped solid-state lasers to generate wavelengths in the blue-green regions of the spectrum. Demonstrations in

1986 of compact green sources based on intracavity frequency doubling of diode-pumped neodymium lasers by researchers at Spectra-Physics and Stanford University sparked tremendous interest in sources based on this approach. This interest has led to commercially-available diode-pumped green sources with powers of several watts and, more recently, blue sources with powers of several milliwatts.

Rather than pump a neodymium laser, why not simply use nonlinear optics to frequency double the output of an infrared semiconductor laser directly? The reason has been, until fairly recently, that high-power semiconductor diode lasers have had rather broad spectral distributions and rather poor spatial beam quality. While these characteristics did not prevent the use of these diode lasers as pumps for solid-state lasers, they did inhibit their use for direct nonlinear frequency conversion, in which the spectral and spatial mode properties of the infrared source are much more critical. As the spatial and spectral mode properties of high-power semiconductor diode lasers have improved, however, the same techniques of nonlinear frequency conversion have been applied to direct frequency-doubling of these devices, and efficient blue and green sources have been demonstrated. In some cases, resonant enhancement and guided-wave geometries have been used to increase the efficiencies of these nonlinear interactions.

An alternative approach to blue-green light generation using infrared sources is the so-called “upconversion laser”. In a standard laser, energy conservation requires that the energy of an absorbed pump photon be greater than the energy of an emitted laser photon; hence the pump wavelength must be shorter than the lasing wavelength. In upconversion lasers, the energy from two or more pump photons is combined to excite the lasing transition; thus the pump wavelength can be longer than the lasing wavelength, so that, for example, infrared light can be used to directly pump a green laser. Although upconversion lasing was demonstrated in 1971 by Johnson and Guggenheim (1971), the field remained largely dormant for several years because flashlamp pumping of such lasers was inefficient. Experiments conducted at IBM in 1986 which demonstrated efficient laser pumping of upconversion lasers revived interest in the field. These initial experiments used bulk rare-earth-doped crystals and had to be performed at cryogenic temperatures, but they demonstrated the feasibility of these devices, including the fact that they could be efficiently pumped with laser diodes. Later, efficient room-temperature operation was achieved using optical fibers doped with rare-earth elements.

Perhaps the most direct and attractive way to generate blue and green light is to use a semiconductor diode laser. Semiconductor laser devices are efficient, small, robust, rugged, and powerful. However, in order to generate blue-green radiation, semiconductors with bandgaps of ~ 3 eV must be used. Suitable materials systems include II–VI semiconductors such as ZnS and ZnSe, and wide-gap III–V materials such as GaN. The growth of thin films of these semiconductors suitable

for device fabrication has proven to be an extremely difficult challenge. However, breakthroughs in the growth of appropriately-doped films in both material systems has allowed the demonstration of light-emitting diodes (LEDs) and, more recently, lasers in both material systems. However, despite rapid progress, demonstration of continuous-wave (cw) operation at room temperature with powers and lifetimes comparable to infrared semiconductor lasers has not yet been achieved, and more development is required before these lasers can be used in the applications cited above.

1.2 APPLICATIONS FOR COMPACT BLUE-GREEN LASERS

One of the factors that has made the field of compact blue-green lasers interesting and vibrant is its diversity in both the variety of technical approaches used to produce them and the wide range of applications for which they have been sought. The specialized topical meetings that sprang up in the early 1990s in response to the intense interest and activity in this field (such as the Optical Society of America's Topical Meeting on Compact Blue-Green Lasers, held in 1992, 1993, and 1994) brought together researchers from such disparate fields as submarine communications and DNA sequencing. In this section, we review some of the principal applications for which blue-green lasers have been sought, and the requirements placed on the lasers by these uses.

1.2.1 Optical data storage

The terms "optical data storage" and "optical recording" have been used to refer to a variety of different approaches for recording and retrieving information using optical methods, including those based on such exotic phenomena as persistent spectral hole burning (Lenth *et al.*, 1986). However, these terms usually refer to somewhat more mundane systems that read data from (and, in some cases, write data to) spinning disks in a fashion analogous to magnetic disk drives (Figure 1.1).

In optical data storage systems, a bit is stored on the disk by altering some physical characteristic of the disk in a tiny spot. This alteration can be done once, as in the case of read-only disks (such as audio CDs and CD-ROMs), or it can be done repeatedly, as in the case of rewritable disks (such as those based on magneto-optic or phase-change media). To read back the information stored on an optical disk, a focused laser beam is scanned over these spots and the light reflected from the disk is detected. The physical characteristic that was altered to record a bit must produce a corresponding change in some optical property of the reflected beam. In audio CDs and CD-ROMs, data are impressed upon a plastic disk in the form of tiny pits stamped into the disk by the manufacturer. The depth of these pits is one-fourth

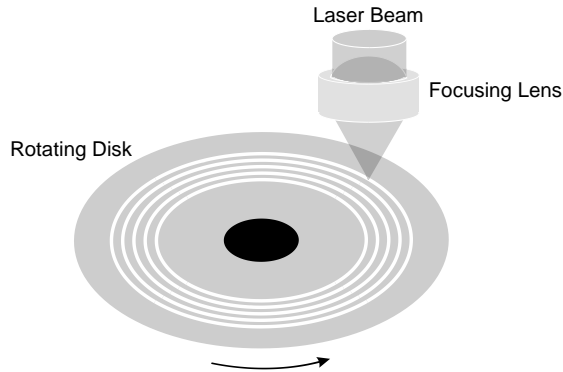


Figure 1.1: Optical data storage system.

the laser wavelength, so that when the beam is scanned over the pit, the portion reflected from the bottom of the pit travels an additional half-wavelength compared with the light reflected from the surface of the disk and is therefore 180° out-of-phase with it; thus, the amplitude of the reflected beam is diminished due to destructive interference. In “magneto-optic” media, data are recorded by using the laser beam as a heater: the focused laser spot heats the magnetic material above the Curie temperature, and the presence of an applied magnetic field causes the magnetization of the medium to reverse in the heated region. When the heating is removed and the material cools below the Curie temperature, that reversed magnetization is “frozen in”. The data can be read back by exploiting the fact that the polarization of light reflected from the disk in these materials depends on the orientation of the magnetic domain (the “polar Kerr effect”). In “phase-change” material, data are recorded by using the focused laser beam to melt the material locally and induce a phase transition from what was originally a crystalline structure to an amorphous one. Data are read back by exploiting the fact that the amorphous state of the material has a different reflectivity than the crystalline state.

In order to write a small mark and be able to read it back accurately, the laser beam must be focused to as small a spot as possible. A gaussian beam can be focused by a lens to a diffraction-limited spot with a diameter d of

$$d \simeq \frac{\lambda}{NA}$$

where λ is the wavelength and NA is the numerical aperture of the lens. Therefore, one way to achieve a smaller spot size is to reduce the wavelength. Halving the wavelength from that of a GaAlAs laser diode at 860 nm to that of a blue laser at 430 nm would cut the spot size in half, and could quadruple the storage density. In addition, for a given rotation rate of the disk, the data rate could be increased by a

factor of 2, since the marks can be placed twice as close together. An additional motivation to pursue development of blue-green lasers for magneto-optic storage was the discovery of garnet-based recording materials that exhibit better performance in the blue-green regions of the spectrum than do their counterparts designed for use in the infrared (Eppler and Kryder, 1995).

Using a blue-green laser in an optical storage system places severe demands upon its performance (Kozlovsky, 1995). In the magneto-optic approach, the power required is comparable with that demanded of the infrared diode lasers used for optical storage (~ 40 mW) (Asthana, 1994). This may seem counterintuitive – one might expect that since the beam is focused to a smaller spot, less power would be required to produce the same temperature increase for writing. This statement is true as far as it goes; however, when reading data back with a blue beam, there are fewer photons per milliwatt than would be present in an infrared beam, which leads to increased noise. In order to obtain an adequate signal-to-noise ratio, the recording medium must be de-sensitized so that a higher readback power can be used without erasing the data. Thus, something like 2–6 mW is required for reading and 40–50 mW are required for writing. For focusing to a small spot, the wavefront aberration of the blue beam must be less than 0.05 wavelengths. The noise of the blue beam must be low: < -110 dBc (decibels below carrier) for magneto-optic storage, where differential detection is used, and < -135 dBc for phase change and CD-ROM, where single-ended detection is used. The laser must have a long lifetime, ideally as long as the lifetime of the drive itself (perhaps 100 000 hours mean-time-between-failures). Finally, the laser must be inexpensive.

1.2.2 Reprographics

Reprographic applications use lasers in a fashion similar to optical data storage – the laser is focused to a small spot and used to make a mark on some medium. Here, however, the medium is the photoconductor of a laser printer, or photographic film or paper. Except in certain specialized applications (for example, writing on microfilm), reprographics does not require as small a spot size as optical data storage. A laser printer with 2400 dpi resolution requires that the laser beam be focused to only a $10\ \mu\text{m}$ spot, a size that can be achieved easily using a red or near-infrared diode laser. However, this $10\ \mu\text{m}$ spot size must be maintained as the beam is scanned rapidly over a page several centimeters wide. Decreasing the wavelength for a particular spot size relaxes the design requirements of the optical system by reducing the numerical aperture required to form a spot of the desired size and by increasing the depth-of-field.

In color reprographics, lasers can be used to expose photographic paper or film (Owens, 1992). The considerations just described for laser printers also apply here.

In addition, the wavelengths of the lasers must be chosen to provide correct exposure for existing photographic media. For photographic films, wavelengths of 430 nm, 550 nm, and 650 nm (blue, green, red) are desired. For photographic papers, wavelengths of 470 nm, 550 nm, and 700 nm are preferred. Powers of a few milliwatts are needed, along with good beam quality, low noise, and high stability. The ability to directly modulate the laser at frequencies up to 50 MHz is desirable.

1.2.3 Color displays

Blue-green lasers have also been sought for use in color displays. At present, the most popular type of color display device is the cathode ray tube (CRT) used in computer monitors and color televisions. In CRTs, colors are synthesized through the superposition of three primary colors – red, green, and blue – generated by an electron beam striking one of three corresponding phosphors. The combination of these red, green, and blue emissions in various proportions creates the other colors visible on the screen. A similar approach has been proposed for laser-based displays, in which three separate lasers would provide red, green, and blue primary colors that could be combined to project full-color images on a large screen (Figure 1.2). Each laser could be raster-scanned across the screen, or could remain stationary and be used to illuminate an “image gate”, such as motion picture film or a spatial light modulator containing the image to be projected.

Lasers are attractive light sources for display applications because of their high brightness and complete color saturation. The brightness of a laser (power emitted per unit area per unit solid angle) can be very high due to the directionality of

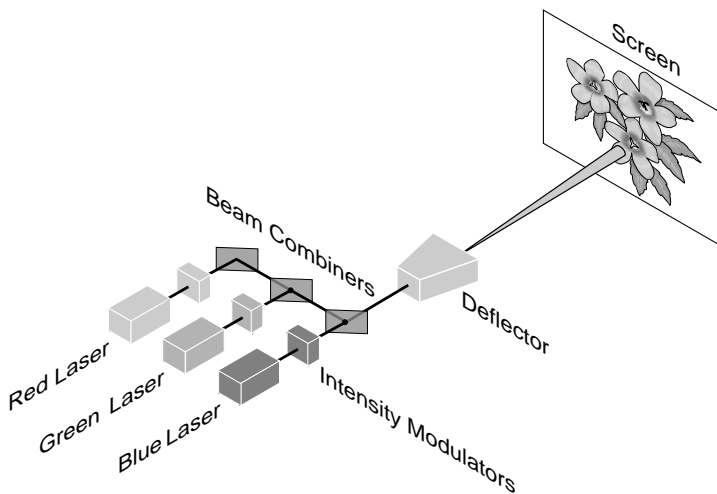


Figure 1.2: Laser-based color projection display.

the beam. This high brightness leads to high efficiency for a laser-based projector, since most of the generated optical power can be directed by appropriate optics to illuminate the screen or image gate. In contrast, a conventional motion picture projector uses an incandescent bulb that emits light into a 4π -steradian solid angle, most of which never reaches the screen. The ability of a laser to concentrate the emitted light into a confined solid angle provides an efficiency advantage over competing technologies (Glenn and Dixon, 1993).

Another advantage of laser-based displays is improved color saturation. In conventional CRT displays, the light emitted by the phosphor is not spectrally pure; the spectral bandwidth of the emission may be several nanometers. In the language of color theory, the red, green, and blue colors emitted by these phosphors are not “fully saturated”: that is, the primary colors are not the “bluest blue”, “greenest green”, or “reddest red” that the eye can perceive, but appear somewhat washed out by the addition of white. As a result, a CRT cannot reproduce the entire range of colors perceptible to human vision, and in particular, cannot produce fully saturated colors. The range of colors that can be produced by addition of primaries can be depicted by the “CIE chromaticity diagram” (Figure 1.3). In this diagram, fully saturated colors (monochromatic light waves of a specified wavelength) correspond to points around the periphery. White corresponds to a point in the interior of the

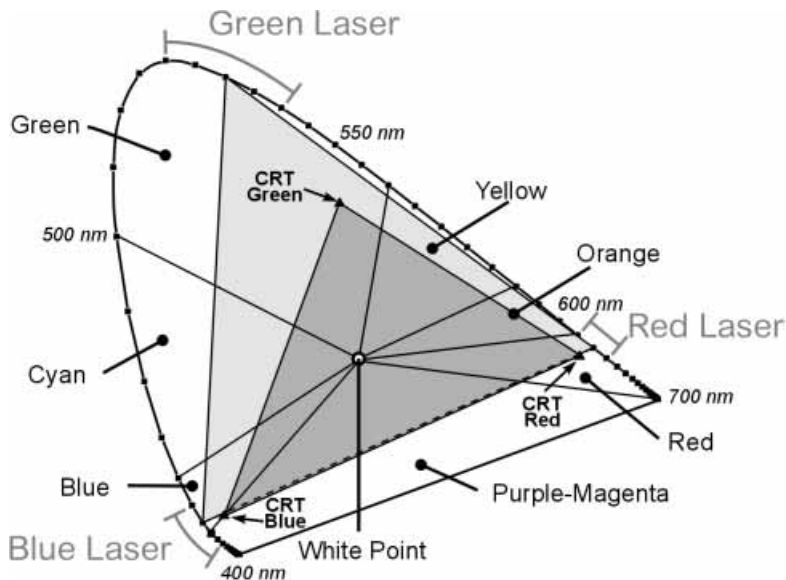


Figure 1.3: CIE diagram showing the color space spanned by CRT phosphors (dark shading) and the color space which could be spanned in a color display using monochromatic red, green, and blue lasers to generate the primary colors (lighter shading). The primary colors for each system fall at the corners of the triangles, as indicated.

diagram. If one draws a line from the “white point” out to a particular color on the periphery, the points along that line represent various saturation levels of the same color; for example, fully saturated green corresponds to a point on the periphery, and points along the line correspond to increasingly paler shades of green as one moves toward the white point. If one plots the points corresponding to three primary colors on such a diagram, the range of colors that can be synthesized by combining these primaries corresponds to the interior of the triangle connecting the three primary points. Figure 1.3 shows the points corresponding to the primary colors of a standard color CRT monitor. Although the red CRT phosphor is nearly saturated, the blue and green phosphors are considerably less so. Thus, while a CRT monitor can produce well-saturated reds, it is difficult to achieve well-saturated blues and greens. A laser-based color display produces primary colors that are fully saturated (that is, spectrally-pure monochromatic waves); thus, the range of colors that can be produced is greater and the colors themselves are richer than in a CRT. In order for the primary colors to appear to human vision as true blues, greens, and reds, they must fall within the wavelength ranges depicted in Figure 1.3: $605 \text{ nm} \pm 5 \text{ nm}$ for red, $530 \text{ nm} \pm 10 \text{ nm}$ for green, and $470 \text{ nm} \pm 10 \text{ nm}$ for blue (Glenn and Dixon, 1993). The power required varies depending upon the size of the screen, but ranges from approximately 1 W per color for a 10-ft \times 16-ft screen to 20 mW per color for a 16-in CRT-like display (Valley and Ansely, 1997).

1.2.4 Submarine communications

Communication with a submerged vessel has been another important application driving the development of blue-green lasers. Naval forces would like to be able to send messages to their submarines without requiring them to rise from their operating depth and risk detection by an enemy (Figure 1.4). Ideally, such a communications system would be able to send a signal through seawater to a great depth and to transmit information at a rapid rate. Electromagnetic radiation can penetrate seawater to a significant depth only at extremely low frequencies (ELFs) ($\lesssim 100 \text{ Hz}$) or in the blue-green portion of the optical spectrum, where minimum attenuation (the “Jerlov Minimum”) occurs for wavelengths between 400 nm and 500 nm (Figure 1.5). Although ELF systems have been built and used to send messages to submarines, systems using ELFs also have extremely low data rates, and in practice, only extremely short messages can be sent. Transmitting with blue-green wavelengths could make it possible to send messages to great depth with much higher data rate than with ELF. However simple this may sound in principle, the development of such a system has presented such great technical challenges that it has been described as “the most complex communications system known to man” (Painter, 1989).

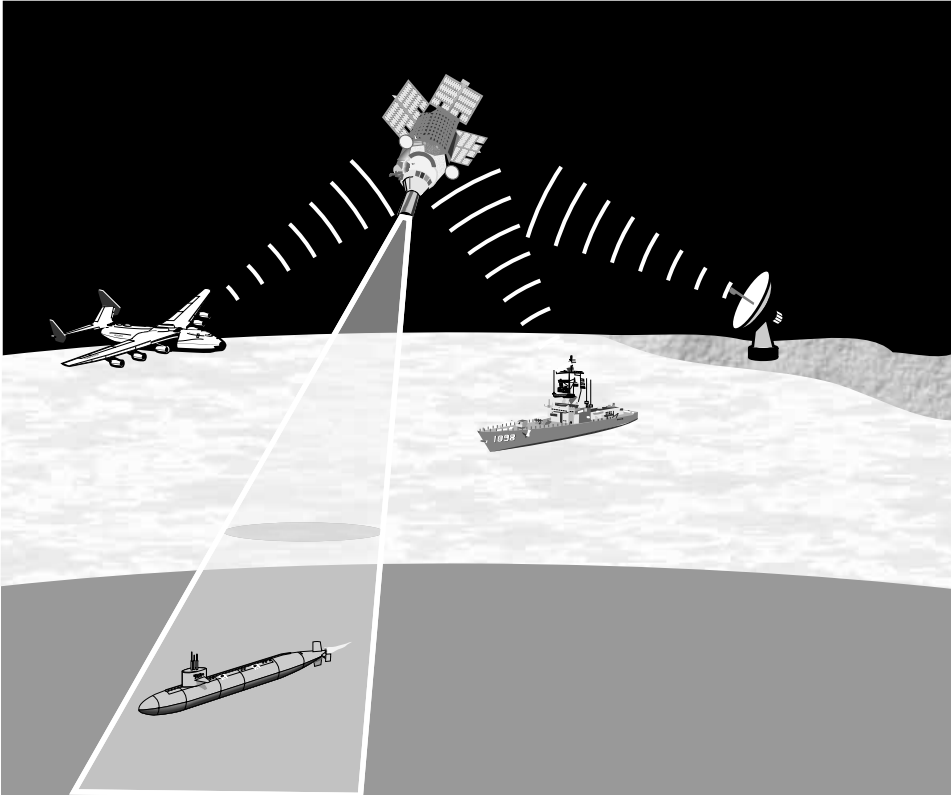


Figure 1.4: Signals are sent by conventional radio from a surface ship, ground station, or aircraft to an orbiting satellite. A blue-green laser aboard the satellite then relays the message to a submerged submarine. (Adapted with permission from Painter (1989).)

What are these challenges? Even at the Jerlov Minimum, the attenuation of seawater is not negligible, and the signal reaching a submerged vessel may be quite weak, requiring the receiver aboard the submarine to be very sensitive. This sensitivity introduces an additional complication: sunlight contains a significant blue-green component which can also penetrate the ocean and introduce noise into the received signal. One way to solve this problem is to exploit the difference between the very narrow spectral width of the blue-green laser and the much broader spectral distribution of sunlight. An optical filter with a sufficiently narrow passband can transmit most of the blue-green laser photons to the detector while rejecting most of the solar photons. In addition to a narrow passband, such a filter must have a wide field-of-view. Photons transmitted from a satellite to a submarine may pass through cloud layers that introduce scattering, and are further scattered during passage through the sea, so that they may impinge upon the submarine from a variety of

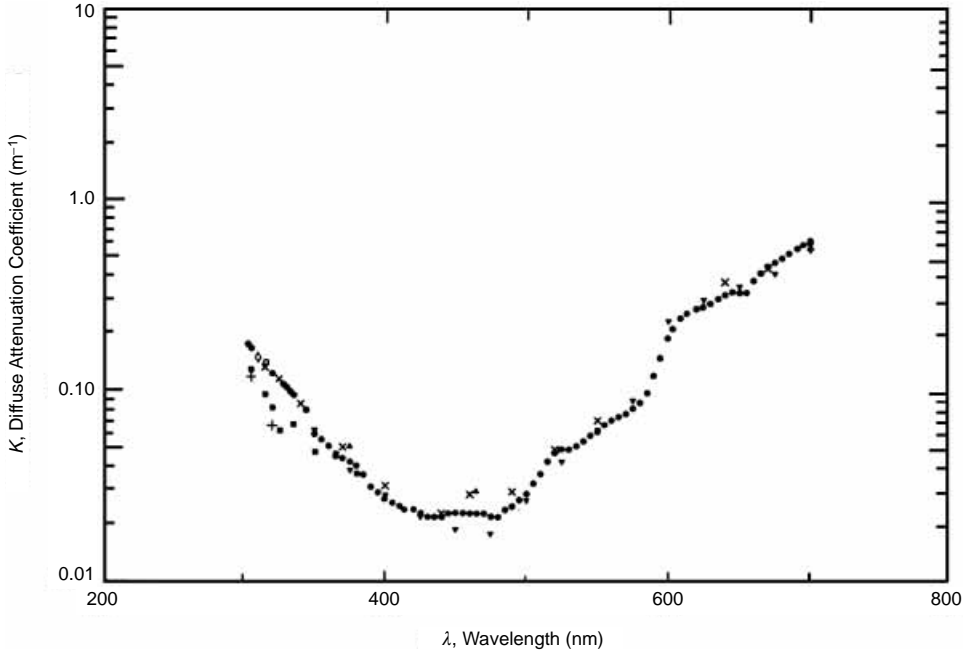


Figure 1.5: Attenuation of seawater over the blue-green portion of the optical spectrum, showing the “Jerlov Minimum” near 450 nm. Various points correspond to measurements by different authors. [Reprinted by permission from Smith and Baker (1981).]

angles. Simultaneously meeting both these requirements – narrow passband and wide field-of-view – is difficult.

The most successful approach devised to meet this challenge is the “atomic resonance filter” or “ARF” (also called “QLORD” – “quantum-limited optical resonance detector”), which has the narrow passband and wide field-of-view required for submarine communications (Gelbwachs, 1988). The ratio of the spectral width $\Delta\lambda$ to center wavelength λ_0 of the passband in these filters can be $\Delta\lambda/\lambda_0 \simeq 10^{-6}$. Thus, for a center wavelength $\lambda_0 \sim 500$ nm, the width of the passband can be as narrow as ~ 0.005 Å (Marling *et al.*, 1979)! An ARF based on cesium vapor is particularly suited to submarine communications and has been pursued for this purpose. The operation of the cesium ARF can be understood from Figure 1.6. A conventional filter (e.g., colored glass such as BG-18) allows only blue-green light to enter the cesium cell. In the cesium vapor, light at 456 nm or 459 nm is absorbed to excite population from the $6s$ level to the $7p$ level. This population subsequently decays nonradiatively to the $6p$ level, through either the $7s$ or $5d$ levels. When the $6p$ population relaxes back to the ground state, infrared photons at 852 nm or 894 nm are emitted. Another conventional filter (such as RG-715 glass) permits only infrared radiation to impinge upon the detector. Since there is no overlap in the passbands of the two conventional filters, no light would reach the detector if the cesium cell

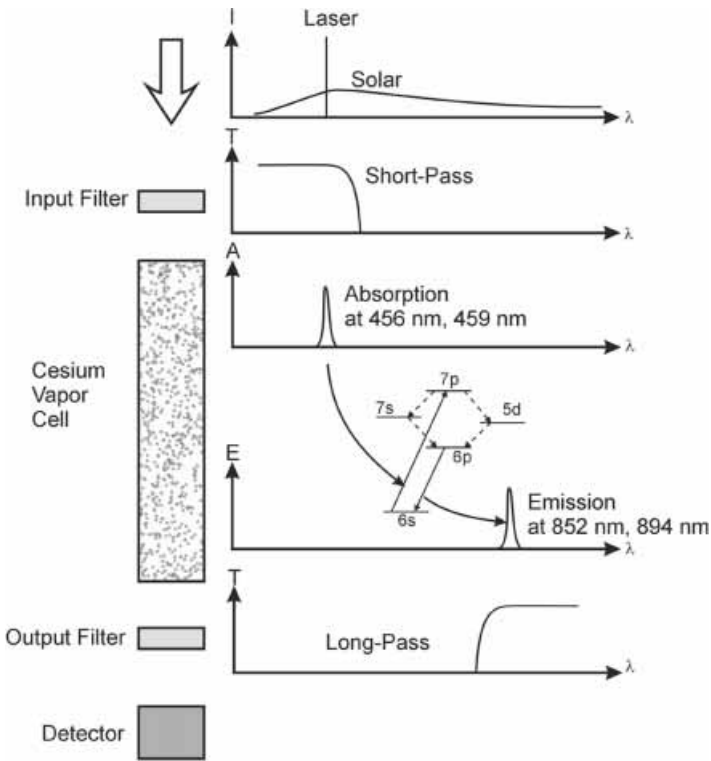


Figure 1.6: Operation of the cesium ARF. I: intensity of incident light, T: transmission of filter, A: absorption of cesium cells, E: emission of cesium cell.

were not present. Thus, the only photons that can impinge upon the detector are those that are converted in wavelength through absorption and reemission by the cesium cell. Since the linewidth of the atomic transition is very narrow, the ARF can have the very narrow passband required for rejection of the solar background and reception of the blue-green laser signal.

However, the same factors which make the cesium filter advantageous for use in submarine communications place stringent requirements upon the blue-green laser. The blue-green laser must be tuned precisely to excite the $6s-7p$ transition; thus, the wavelength must fall within a window approximately 0.01 \AA wide near 456 nm or 459 nm . The narrow spectral width of this transition requires that the laser linewidth be less than $\lesssim 1 \text{ GHz}$ and be stable to the same degree (Leslie, 1995). The required power is in the kilowatt range (*Laser Focus World*, 1980).

The transmission characteristics of seawater also dictate the use of a blue-green laser for a related application: high-resolution optical imaging of the ocean floor (MacDonald *et al.*, 1995). Here, a blue-green laser carried by a moving submarine is scanned across the seafloor perpendicular to the line of travel and the reflected light is collected to create one line of the image. As the submarine moves forward, successive line scans are collected and used to build up a two-dimensional image.

Table 1.1. Ions and wavelengths of interest for laser cooling of trapped ions

Ion	Wavelength	References
Ca	397 nm, 442.7 nm	Urabe <i>et al.</i> (1992), Hayasaka <i>et al.</i> (1994), Beverini <i>et al.</i> (1996)
H	243 nm	Zimmermann <i>et al.</i> (1995)
Mg	383 nm	Beverini <i>et al.</i> (1996)
Pb	368.3 nm	Tamm (1993)
Rb	421 nm	Hemmerich <i>et al.</i> (1990)
Sr	422 nm	Barwood <i>et al.</i> (1992), Barwood <i>et al.</i> (1993)
Yb	369.5 nm	Tamm (1993)

This technique can provide detailed maps of geographical features of the seafloor, or of man-made features such as pipelines.

1.2.5 Spectroscopic applications

Laser cooling of trapped ions is of interest as the basis for optical frequency standards (Itano, 1991). In this approach, an ion is held in an electromagnetic trap and cooled using radiation pressure from a laser slightly detuned from an absorption transition. Several ions that have been proposed for this application require a ultra-violet or blue laser for excitation of the relevant transition (Table 1.1). Convenient sources in the 300–500 nm spectral range are therefore useful for spectroscopy and laser pumping of such transitions. In most cases, relatively modest powers are required (at most, a few milliwatts), but the blue output must be tunable.

A spectroscopic use of blue-green lasers with great immediate practical application is *in situ* process control of physical vapor deposition (PVD). A number of technologically important materials are deposited in thin films from a vapor state, using techniques such as evaporation and sputtering. The deposition rate of these materials is typically measured using a quartz crystal monitor or ion gauge. However, these techniques are not well suited to the deposition requirements of many modern, technologically-important materials. For example, traditional rate-monitoring techniques are inadequate for deposition of superconducting films, in which a high background pressure of oxygen is required, and for co-deposition of composite or alloy films, in which it is necessary to simultaneously monitor and control the flux of more than one species. In addition, these monitoring techniques require physically placing a sensor within the deposition chamber. Since the sensor must not obscure the target, or otherwise interfere with deposition of materials on it, it necessarily cannot directly measure the characteristics of the flux incident upon the substrate.

An alternative technique for monitoring the evaporation flux is atomic absorption spectroscopy. In this approach, a laser beam is passed through the atomic vapor and

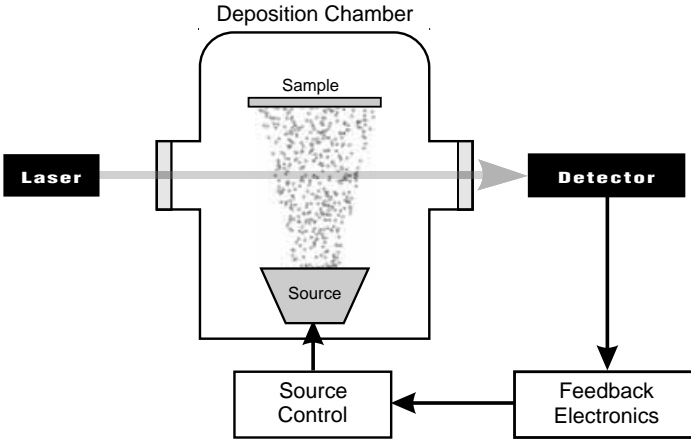


Figure 1.7: A tunable blue-green laser is used for monitoring and controlling the deposition rate in a PVD system.

is tuned to an absorption line (Figure 1.7). The beam is attenuated by absorption in the vapor and the emerging intensity is given by Beer's law, $I = I_0 e^{-n\sigma l}$, where I_0 is the initial intensity, I is the output intensity, n is the density of the evaporant, σ is the absorption cross-section, and l is the path length. By measuring the effect of the atomic vapor on the intensity of the transmitted laser beam, the evaporation rate can be determined. In addition, this information can be fed back to the vapor source and used for closed-loop control of the evaporation rate. Unlike other techniques for monitoring evaporation rate, atomic absorption spectroscopy is noninvasive, can be used with unusual deposition geometries, is highly sensitive and species selective, and can probe both the spatial and velocity distribution of the evaporant.

Atomic absorption spectroscopy can be implemented using hollow cathode lamps; however, these lamps have a number of unattractive features, including relatively short lifetime (~ 1000 h), low intensity, and broad spectral width (Benerofe *et al.*, 1994). The use of a laser instead of a hollow cathode lamp offers several advantages: long lifetime, high intensity, and narrow spectral width can be obtained. Because the linewidth of the laser can be very narrow, Doppler broadening of the evaporated flux can be investigated. Sophisticated spectroscopic techniques, such as frequency-modulation spectroscopy (Bjorklund, 1980) or nonlinear spectroscopy (Levenson, 1982) can be employed.

There are several technologically-important materials that are deposited by PVD and that have absorption lines in the blue-green portion of the spectrum, including: aluminum (394 nm) (Wang *et al.*, 1996), titanium (391 nm) (Galanti *et al.*, 1996), yttrium (408 nm) (Wang *et al.*, 1995), tungsten (385 nm), and gallium (403 nm). Again, the laser must be tunable over the relevant absorption line and powers on the order of a milliwatt are required.

1.2.6 Biotechnology

Blue-green lasers also have uses in the field of biotechnology (Trainor, 1990). One of the most important applications is flow cytometry, in which cells that have certain properties are counted or measured as they are forced to flow by a detector. Cells with the desired property can be detected by attaching to them a fluorescent molecule, or “fluorophore.” The flowing cells are forced to pass through the focused beam of a laser that is tuned to excite the fluorophore, and the presence of the cell can be detected by looking for the associated fluorescence.

One particularly important example of flow cytometry is DNA sequencing. The objective of this procedure is to determine the sequence of the four nucleotides (adenosine, cytosine, guanosine, and thymidine) that encode genetic information in the molecular structure of DNA. Such sequences are important for understanding and diagnosing human genetic disorders and for examining forensic evidence in criminal cases. In one technique for DNA sequencing, a portion of the code is determined by creating a series of replicas of a particular section of the DNA molecule. Each replica starts at the same point in the sequence, but differs in length from the other replicas by one nucleotide (Figure 1.8). Thus, if the replicas can be sorted by length and if the terminal nucleotide can be determined, the DNA sequence can be deduced.

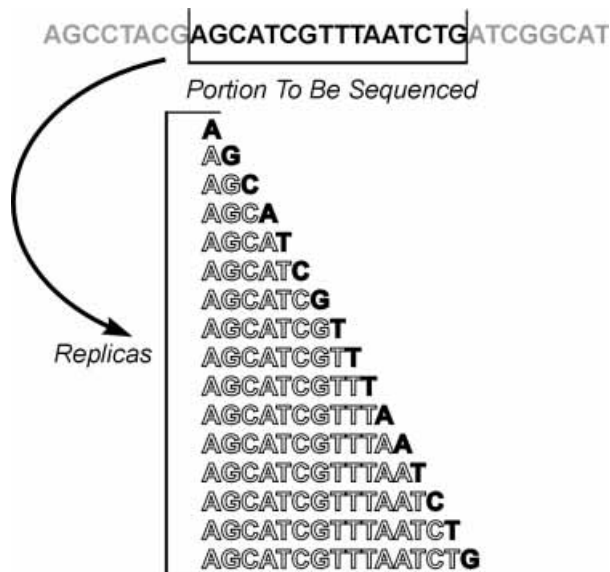


Figure 1.8: A portion of the DNA sequence is determined by making a series of replicas, each of which differs by one nucleotide in length. If the replicas can be sorted by length, and the terminating nucleotide can be determined, then that portion of the DNA sequence can be reconstructed.

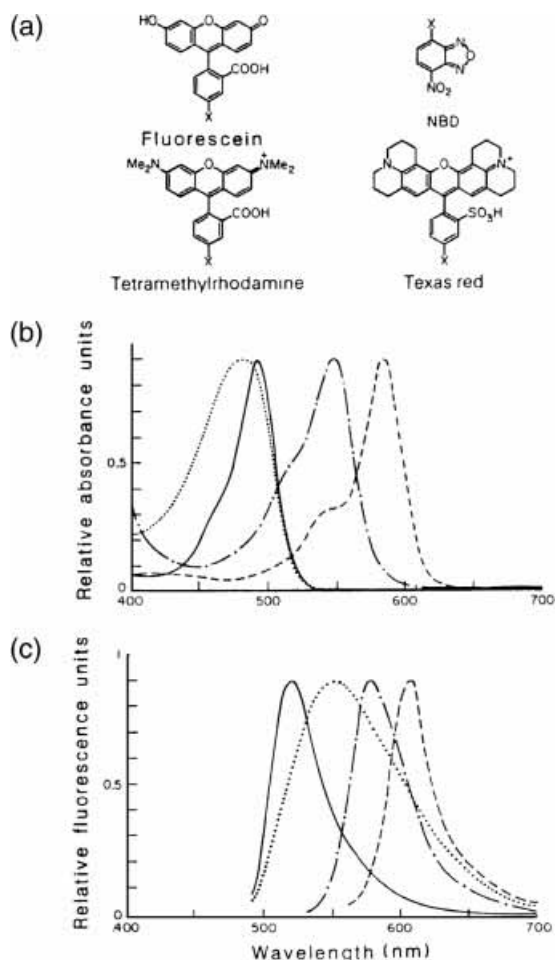


Figure 1.9: (a) Four dyes used for tagging DNA nucleotides. (b) The corresponding absorption spectra. Solid curve: fluorescein; dotted curve: NBD; dashed curve: Texas Red; dot-dash curve: tetramethylrhodamine. (c) The corresponding fluorescence spectra. Same line types as in (b). (Reprinted with permission from Smith *et al.* (1986). Copyright: Macmillan Magazines Limited.)

The terminating nucleotide of each replica can be determined by “tagging” the replica with one of four fluorophores, each fluorophore marking the presence of one of the four possible nucleotides. The fluorophores are chosen such that their emission peaks are sufficiently separated to be easily resolved and identified. Four common fluorescent molecules used for this purpose are shown in Figure 1.9, together with their absorption and emission spectra (Smith *et al.*, 1986). All of these dyes can be excited using blue-green wavelengths.

The replicas can be sorted by length by forcing them to diffuse through an electrophoresis cell. Longer replicas move more slowly than short ones; thus, the

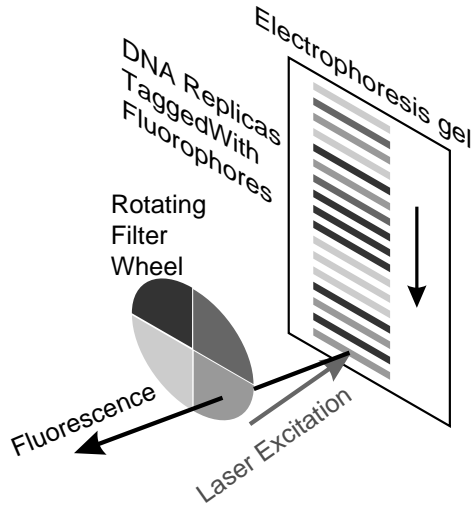


Figure 1.10: DNA replicas are sorted by diffusion through an electrophoresis cell. The nucleotide terminating each replica is tagged with a fluorophore. As each replica reaches the end of the gel, excitation from a blue-green laser excites emission from the fluorophore. The fluorophore and corresponding nucleotide are identified by analyzing the fluorescent emission through a filter wheel. (Adapted with permission from Trainor (1990). Copyright: American Chemical Society.)

replicas become spatially separated as they pass through the cell, spreading out like runners of different speeds in a race (Figure 1.10). This spatial separation corresponds to a temporal one; each replica crosses the “finish line” at a different time. This spatial/temporal separation is remarkably linear with respect to the length of the replica, and replicas that differ by only one nucleotide in length can be easily distinguished. As each replica reaches the end of the gel, it passes through a focused blue-green laser beam. The blue-green photons are absorbed by the fluorophore, which then fluoresces, emitting photons at its own characteristic wavelength. The fluorophore can then be identified by analyzing the spectral content of the emitted photons; this can usually be done simply with a filter wheel divided into four sections, each of which passes only the signal associated with one particular fluorophore.

A great deal of development and engineering has gone into DNA sequencers based on this technology, and several commercial products are available that use argon-ion lasers as the source of blue-green light. Hence, for compatibility with existing products, manufacturers of DNA sequencers and other flow cytometry instrumentation seek compact blue-green lasers operating at wavelengths of 488 nm and 514 nm. The powers required can be as low as 10 mW and as high as several watts, depending on the details of the application (Sklar, 1992).

1.3 BLUE-GREEN AND BEYOND

In addition to the representative applications discussed above, there are numerous others – including straightforward, but commercially important ones (such as CD mastering (Kaneda and Kubota, 1997) and semiconductor wafer inspection) and rather exotic ones (such as calibration of neutrino detectors (Kitchin and Newcomer, 1994)). These all exploit some property of blue-green light in much the same way as those applications we have already discussed.

In addition, the technologies explored for compact blue-green light generation border on other fields where identical ideas are employed, even if generation of blue-green light is not the primary objective. For example, efficient nonlinear frequency-doubling of near-infrared light in resonators (Pereira *et al.*, 1988) and waveguides (Anderson *et al.*, 1995) has been of great interest in the production and study of squeezed states. The same ideas used in upconversion lasers have been applied to three-dimensional displays based on exciting visible fluorescence by absorption of two infrared photons in a volume element defined by the intersection of two diode laser beams in a cube of rare-earth-doped glass (Downing *et al.*, 1996). The development of efficient blue LEDs based on II–VI and III–V semiconductors has been both a precursor to the development of lasers based on the same technology and an important end in itself, as there are many applications for which LEDs are preferred over lasers.

Finally, the topics discussed in the remainder of this book – the basics of second-order nonlinear processes, materials for second-harmonic generation and sum-frequency mixing, diode-pumping and intracavity frequency doubling of solid-state lasers, nonlinear frequency conversion in resonators and waveguides, rare-earth spectroscopy and the physics of upconversion lasers, and fundamentals of semiconductor diode lasers – are relevant to the generation of wavelengths other than blue-green ones. There is great interest in compact sources of light in portions of the visible spectrum other than the blue-green, and in the generation of wavelengths longer than $\sim 1 \mu\text{m}$ using near-infrared semiconductor and diode-pumped solid-state lasers as the starting point. Many of the basic ideas used for upconversion of near-infrared light to shorter wavelengths (particularly those based on nonlinear optics) can also be used for downconversion to longer wavelengths. The fundamentals outlined in the remainder of this book should establish a sound basis for understanding these devices as well.

REFERENCES

- Anderson, M. E., Beck, M., Raymer, M. G., and Bierlein, J. D. (1995) Quadrature squeezing with ultrashort pulses in nonlinear waveguides. *Opt. Lett.*, **20**, 620–622.

- Asthana, P. (1994) Laser diodes must meet tight specs for magneto-optical data storage. *Laser Focus World*, January, 123–125.
- Barwood, G. P., Edwards, C. S., Gill, P., Klein, H. A., and Rowley, W. R. C. (1992) Development of diode and fibre laser sources for a Sr^+ trapped ion optical frequency standard. *Proc. SPIE*, **1837**, 271–277.
- Barwood, G. P., Edwards, C. S., Gill, P., Klein, H. A., and Rowley, W. R. C. (1993) Observation of the $5s\ ^2S_{1/2} - 4d\ ^2D_{5/2}$ transition in a single laser-cooled trapped Sr^+ ion by using an all-solid-state system of lasers. *Opt. Lett.*, **18**, 732–734.
- Benerofe, S. J., Ahn, C. H., Wang, M. M., Kihlstrom, K. E., Do, K. B., Arnason, S. B., Fejer, M. M., Geballe, T. H., Beasley, M. R., and Hammond, R. H. (1994) Dual beam atomic absorption spectroscopy for controlling thin film deposition rates. *J. Vac. Sci. Technol. B.*, **12**, 1217–1220.
- Beverini, N., Maccioni, E., Strumia, F., Godone, A., and Novero, C. (1996) Frequency doubled laser diodes: Application to Mg and Ca atomic frequency standards. *Laser Phys.*, **6**, 231–236.
- Bjorklund, G. C. (1980) Frequency-modulation spectroscopy: a new method for measuring weak absorptions and dispersions. *Opt. Lett.*, **5**, 15–17.
- Downing, E. A., Hesselink, L., Macfarlane, R. M., Klein, J. R., Evans, D., and Ralson, J. (1996) A laser-diode-driven, three-color, solid-state 3-D display. In *Conference on Lasers and Electro-Optics*, Vol. 9, 1996 OSA Technical Digest Series, pp. 89–90. Washington: Optical Society of America.
- Eppler, W. R. and Kryder, M. H. (1995) Garnets for short wavelength magneto-optic recording. *J. Phys. Chem. Solids*, **56**, 1479–1490.
- Galanti, S. A., Berzins, L. V., Brown, J. B., Tamosaitis, R. S., Bortz, M. L., Day, T., Fejer, M. M., and Wang, W. (1996) Demonstration of a vapor density monitoring system using UV radiation generated from quasi-phasematched SHG waveguide devices. *Proc. SPIE*, **2700**, 334–347.
- Gelbwachs, J. A. (1988) Atomic resonance filters. *IEEE J. Quant. Electron.*, **24**, 1266–1277.
- Glenn, W. E., and Dixon, G. J. (1993) Bright future projected for lasers in electronic cinemas. *Laser Focus World*, November, 73–80.
- Hayasaka, K., Watanabe, M., Imajo, H., Ohmukai, R., and Urabe, S. (1994) Tunable 397-nm light source for spectroscopy obtained by frequency doubling of a diode laser. *Appl. Opt.*, **33**, 2290–2293.
- Hemmerich, A., McIntyre, D. H., Zimmermann, C., and Hänsch, T. W. (1990) Second-harmonic generation and optical stabilization of a diode laser in an external ring resonator. *Opt. Lett.*, **15**, 372–374.
- Itano, W. M. (1991) Atomic ion frequency standards. *Proc. IEEE.*, **79**, 936–942.
- Johnson, L. F., and Guggenheim, H. J. (1971) Infrared-pumped visible laser. *Appl. Phys. Lett.*, **19**, 44–47.
- Kaneda, Y., and Kubota, S. (1997) CW Solid-state ultraviolet laser for optical disk mastering application. *IEEE J. Sel. Top. Quantum Electron.*, **3**, 35–39.
- Kitchin, P. J. and Newcomer, F. M. (1994) Feasibility of a frequency-doubled, pulsed GaAs laser diode source for calibration of photomultipliers at the Sudbury Neutrino Observatory. In *Proceedings of the 1993 IEEE Nuclear Science Symposium and Medical Imaging Conference*, Pt. 1, pp. 686–690. IEEE.
- Kozlovsky, W. (1995) Optical data storage requirements on short wavelength laser sources. *Proc. SPIE*, **2379**, 186–190.
- Laser Focus World* (1980) Blue-green laser links to subs., April, 14–18.

- Lenth, W., Macfarlane, R. M., Moerner, W. E., Schellenberg, F. M., Shelby, R. M., and Bjorklund, G. C. (1986) High-density frequency-domain optical recording. *Proc. SPIE*, **695**, 216–223.
- Leslie, K. R. (1995). Alexandrite solid state blue laser. *Proc. SPIE*, **2380**, 82–87.
- Levenson, M. D. (1982) *Introduction to Nonlinear Laser Spectroscopy*. New York: Academic Press.
- MacDonald, I. R., Chu, J. S., Reilly, J. F., Blincow, M., and Olivier, D. (1995) Deep-ocean use of the SM2000 laser line scanner on submarine NR-1 demonstrates system potential for industry and basic science. *Challenges Of Our Changing Global Environment: Oceans 95*, 555–565.
- Marling, J. B., Nilsen, J., West, L. C., and Wood, L. L. (1979). An ultrahigh-Q isotropically sensitive optical filter employing atomic resonance transitions. *Appl. Phys. Lett.*, **50**, 610–614.
- Owens, J. C. (1992) Compact visible lasers in reprographics. In *Compact Blue Green Lasers Technical Digest 1992*, Vol. 6, pp. 8–9. Washington: Optical Society of America.
- Painter, Floyd C. (1989) Submarine laser communications. *Defense Electronics*, June, 82–94.
- Pereira, S. F., Xiao, Min, Kimble, H. J., and Hall, J. L. (1988) Generation of squeezed light by intracavity frequency doubling. *Phys. Rev. A.*, **38**, 4931–4934.
- Sklar, L. A. (1992) Lasers in flow cytometry and biotechnology. In *Compact Blue Green Lasers Technical Digest 1992*, Vol. 6, pp. 5–7. Washington: Optical Society of America.
- Smith, L. M., Sanders, J. Z., Kaiser, R. J., Hughes, P., Dodd, C., Connell, C. R., Heiner, C., Kent, S. B. H., and Hood, L. E. (1986) Fluorescence detection in automated DNA sequence analysis. *Nature*, **321**, 674–679.
- Smith, R. C., and Baker, K. S. (1981) Optical properties of the clearest natural waters (200–800 nm). *Appl. Opt.*, **20**, 177–184.
- Tamm, C. (1993) A tunable light source in the 370 nm range based on an optical stabilized, frequency-doubled semiconductor laser. *Appl. Phys. B.*, **56**, 295–300.
- Trainor, G. L. (1990) DNA sequencing, automation, and the human genome. *Anal. Chem.*, **62**, 418–426.
- Urabe, S., Watanabe, M., Imajo, H., and Hayasaka, K. (1992) Laser cooling of trapped Ca^+ and measurement of the $3\ ^2\text{D}_{5/2}$ state lifetime. *Opt. Lett.*, **17**, 1140–1142.
- Valley, G. and Ansley, D. (1997) Private communication.
- Wang, W., Hammond, R. H., Fejer, M. M., Ahn C. H., Beasley, M. R., Levenson, M. D., and Bortz, M. L. (1995) Diode-laser-based atomic absorption monitor using frequency modulation spectroscopy for physical vapor deposition process control. *Appl. Phys. Lett.*, **67**, 1375–1377.
- Wang, W., Fejer, M. M., Hammond, R. H., Beasley, M. R., Ahn, C. H., Bortz, M. L. and Day, T. (1996) Atomic absorption monitor for deposition process control of aluminum at 394 nm using frequency-doubled diode laser. *Appl. Phys. Lett.*, **68**, 729–731.
- Zimmermann, C., Vuletic, V., Hemmerich, A. and Hänsch, T. W. (1995) All solid state laser source for tunable blue and ultraviolet radiation. *Appl. Phys. Lett.*, **66**, 2318–2320.